

## A study of the Carboxyethylimidazoline as an H<sub>2</sub>S Corrosion Inhibitor of X-120 Pipeline Steel

E.F. Diaz<sup>1</sup>, J.G. Gonzalez-Rodriguez<sup>2</sup>, R. Sandoval-Jabalera<sup>3</sup>, S. Serna<sup>2</sup>, B. Campillo<sup>4</sup>, M.A. Neri-Flores<sup>1</sup>, C. GaonaTiburcio<sup>1</sup>, A. Martinez-Villafañe<sup>1\*</sup>

<sup>1</sup> Centro de Investigacion en Materiales Avanzados, Miguel de Cervantes 120, Chihuahua. Chih. Mexico

<sup>2</sup> Universidad Autónoma del Estado de Morelos-C.I.I.C.Ap, Av. Universidad 1001, 6225-Cuernavaca, Mor., Mexico

<sup>3</sup> Universidad Autónoma de Chihuahua, Facultad de Ingeniería. Chihuahua, Chih. México

<sup>4</sup> Instituto de Ciencias Físicas-Facultad de Química-Universidad Nacional Autónoma de México, Cuernavaca, Mor., México

\*E-mail: [Martinez.villafane@cimav.edu.mx](mailto:Martinez.villafane@cimav.edu.mx)

Received: 10 September 2010 / Accepted: 15 October 2010 / Published: 1 December 2010

---

The H<sub>2</sub>S corrosion inhibition of X-120 pipeline steel by using carboxyethylimidazoline has been evaluated by using electrochemical techniques. Electrochemical techniques include polarization curves, linear polarization resistance, electrochemical impedance spectroscopy and electrochemical noise measurements. Testing solutions includes H<sub>2</sub>S-containing 3% NaCl with different inhibitor concentrations (0, 16, 32, 80, 160 and 332 μmol l<sup>-1</sup>) at 50 °C. Different techniques have shown that by adding 160 μmol l<sup>-1</sup> of carboxyethylimidazoline the susceptibility to both uniform and localized corrosion decreases.

---

**Keywords:** Sour corrosion, corrosion inhibitor, X-120 steel, electrochemical noise.

### 1. INTRODUCTION

Because of its importance in several industries, corrosion of steel in hydrogen sulfide (H<sub>2</sub>S)-containing solutions is a well-known phenomenon that has been investigated for many years. One of these industrial processes is oil and gas production and transport. Produced fluids include CO<sub>2</sub>, H<sub>2</sub>S and chlorides that in combination with water make these media highly corrosive [1, 2]. Oilfield corrosion manifests itself in several forms, among which CO<sub>2</sub> corrosion (sweet corrosion) and hydrogen sulfide (H<sub>2</sub>S) corrosion (sour corrosion) in the produced fluids and corrosion by chloride and oxygen dissolved in water injection are by far the most prevalent forms of attack found in oil and gas

production [3]. Recently, H. Ma et al. [4] found that H<sub>2</sub>S can either accelerate or inhibit corrosion of iron under different experimental conditions such as H<sub>2</sub>S concentration and solution pH. The inhibition effect of H<sub>2</sub>S is attributed to the formation of an FeS protective film for H<sub>2</sub>S concentrations below 40 μmol cm<sup>-3</sup>. Similarly, Abelev et al. [5] has examined the effect of H<sub>2</sub>S at ppm level concentrations on iron corrosion in 3 wt.% NaCl solutions saturated with CO<sub>2</sub> in the temperature range of 25–85 °C using electrochemical and surface science techniques. Small H<sub>2</sub>S concentrations (5 ppm) have an inhibiting effect on corrosion in presence of CO<sub>2</sub> at temperatures from 25 to 55 °C. At 85 °C, however, 50 ppm H<sub>2</sub>S is needed to provide significant corrosion inhibition. At higher H<sub>2</sub>S concentrations, the corrosion rate rapidly increases, while still remaining below the rate for the H<sub>2</sub>S-free solution. Similarly, El-Maksoud [6] studied the behaviour of steel in acidic media. Factors affect the inhibition efficiency of the organic compounds in acidic media were discussed; the effect of the structure, the effect of zero- charge potential and the effect of synergistic effect. Different additives of organic compounds with different active centers were used to prevent corrosion in acidic solutions. Thus, these research works reports a peaking effect of inhibitor concentration ascribed to the formation of an inhibitive film which then breaks down at higher concentrations. Dislike these works, Tang et al. [7] has studied the electrochemical behavior of SAE-1020 carbon steel in 0.25 M Na<sub>2</sub>SO<sub>4</sub> solution containing different concentrations of H<sub>2</sub>S at 90 °C using weight loss, electrochemical measurements, scanning electron microscopy (SEM) and X-ray diffraction (XRD) techniques. Results have shown that the corrosion rate of carbon steel increases significantly with the increase of H<sub>2</sub>S concentration. H<sub>2</sub>S accelerates the corrosion rate of SAE-1020 carbon steel by a promoted hydrogen evolution reaction.

Because of its implications in different industries, corrosion of steel in H<sub>2</sub>S-containing solutions is a well-known phenomenon that has been investigated during many years [7, 8]. The injection of corrosion inhibitor is a standard practice in oil and gas production systems to control internal corrosion of carbon steel structures. Nitrogen-based organic inhibitors such as imidazolines or their salts have been successfully used in these applications even without an understanding of the inhibition mechanism [9-10]. The corrosion inhibition of organic compounds is related to their adsorption properties which depend on the nature and the state of the metal surface, the type of corrosive environment and the chemical structure of the inhibitor [11-13].

Among the different electrochemical techniques that can be used to evaluate inhibitors, electrochemical impedance spectroscopy (EIS) appears as a powerful tool for the information that it can provide, in addition to traditional techniques such as polarization curves or linear polarization resistance (LPR) measurements. However, electrochemical noise (EN) measurements have also been successfully applied to the study performance of corrosion inhibitors [14-18]. These measurements are made without any external perturbation of the system, and provide information of the actual system being studied with little possibility of artifacts due to the measurement technique.

EN technique involves the estimation of the electrochemical noise resistance,  $R_n$ , which is calculated as the standard deviation of potential,  $\sigma_v$  divided by the standard deviation of current  $\sigma_i$ ,

$$R_n = \sigma_v / \sigma_i \quad [1]$$

where  $R_n$  can be taken as the linear polarization resistance,  $R_p$  in the Stern-Geary equation

$$I_{corr} = \frac{b_a b_c}{2.3(b_a + b_c) R_p} \quad [2]$$

thus, inversely proportional to the corrosion rate,  $I_{corr}$ , but with the necessary condition that a trend removal has to be applied over an average baseline as previously established [19]. It has been demonstrated that the noise signal contains information about the dynamics that occur on the surface of the electrode, giving information about the type of corrosion that is occurring, either uniform or localized. Thus, the aim of this work is to study the performance of a simple organic compound, carboxyethylimidazoline, as an  $H_2S$  corrosion inhibitor of API X-120 pipeline steel by using different electrochemical techniques such as polarization curves, LPR, EIS and, particularly, EN measurements.

## 2. EXPERIMENTAL PROCEDURE

### 2.1. Testing material

Material tested was an API X-120 with a chemical composition as given in table 1.

**Table 1.** Chemical composition of X-120 pipeline steel / wt.%.

C	Si	Mn	P	S	Cr	Mo	Ni	Al	Co
0.027	0.24	1.00	0.003	0.004	0.42	0.18	1.35	0.045	0.004
Cu	Nb	Ti	Fe						
0.010	0.024	0.015	96.6						

Slab samples were heated at 1250 °C, increasing the temperature from room temperature at a rate of 0.4 °C s<sup>-1</sup>, soaked during 90 minutes and immediately hot rolled. Initially slab rough rolling was done in five passes within 1250-1098 °C range. Then, the rough rolling was followed by a cooling period until an experimental initial temperature for the final rolling procedure of 1051 °C was reached. A finishing total deformation of 37 % was achieved also in five passes ending at 867 °C. The second and third cooling procedures were performed from 867 during 30 minutes and then water quenched resulting in an acicular ferrite + martensitic microstructure. Cubic specimens measuring 1.0 cm in length with a copper wire welded to make electric contact were cut, embedded in epoxy resin, with an exposed area of 1.0 cm<sup>2</sup>, abraded with 600 grade emery paper, rinsed with distilled water, acetone, and dried under an air flow.

### 2.2. Testing solution

Inhibitor used in this work was a commercial carboxyethylimidazoline with a general structure as shown on Fig. 1, which is composed of a five member ring containing nitrogen elements, a C-14

saturated hydrophobic head group and a pendant, hydrophilic carboxyamido group attached to one of the nitrogen atoms. Inhibitor was dissolved in pure 2-propanol. Concentrations of the inhibitor used in this work were 0, 16, 32, 80, 160 and 332  $\mu\text{mol l}^{-1}$  and the temperature kept constant at 50 °C with a hot plate. The testing solution consists of 3% NaCl solution, heated, de-aerated with nitrogen gas, and  $\text{H}_2\text{S}$  was produced by reacting 3.53  $\text{mg l}^{-1}$  sodium sulfide ( $\text{Na}_2\text{S}$ ) with 1.7  $\text{mg l}^{-1}$  acetic acid. Inhibitor was added 2 hours after pre-corroding the specimen by using a micro syringe.

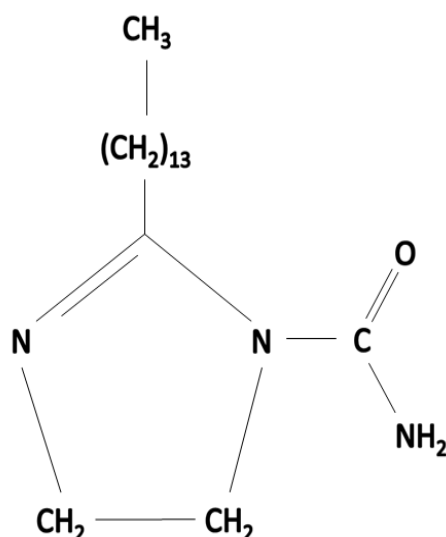


**Figure 1.** General structure of carboxyethylimidazoline.

### 2.3 Electrochemical measurements

Electrochemical techniques employed included potentiodynamic polarization curves, linear polarization resistance (LPR), electrochemical impedance spectroscopy (EIS), and electrochemical noise (EN) measurements in both current and voltage. Measurements were obtained by using a conventional three electrodes glass cell with two graphite electrodes symmetrically distributed and a saturated calomel electrode (SCE) as reference with a Lugging capillary bridge. Polarization curves were recorded at a constant sweep rate of 1  $\text{mV s}^{-1}$  within an interval of  $\pm 300 \text{ mV}_{\text{SCE}}$  with respect to the open circuit potential value,  $E_{\text{corr}}$ . Corrosion current density values,  $I_{\text{corr}}$ , were calculated by using the Tafel extrapolation method and by taking an extrapolation interval of  $\pm 250 \text{ mV}_{\text{SCE}}$  around the  $E_{\text{corr}}$  value once stable. Inhibitor efficiency,  $\eta$ , was calculated as follows

$$\eta (\%) = (I_{\text{corr}} - I'_{\text{corr}}) / I_{\text{corr}} \times 100 \quad [3]$$

where  $I'_{\text{corr}}$  and  $I_{\text{corr}}$  are the corrosion current with and without inhibitor respectively. LPR measurements were carried out by polarizing the specimen  $\pm 10 \text{ mV}_{\text{SCE}}$  with respect to  $E_{\text{corr}}$ , at a scanning rate of 1  $\text{mV s}^{-1}$  every 20 minutes during 24 hours. EIS tests were carried out at the open circuit potential value by using a signal with amplitude of 10  $\text{mV}_{\text{SCE}}$  and a frequency interval of 0.1

Hz-30 kHz. An ACM potentiostat controlled by a desk top computer was used for the LPR tests and polarization curves, whereas for the EIS measurements, a model PC4 300 Gamry potentiostat was used. Finally, EN measurements in both current and potential were recorded using two identical working electrodes and a reference electrode (SCE). Electrochemical noise measurements were made recording simultaneously the potential and current fluctuations at a sampling rate of 1 point per second for a period of 1024 seconds. For the readings in current, two identical working electrodes with the same exposed area were used, whereas for the readings in potential, a SCE electrode was used. A fully automated zero resistance ammeter (ZRA) from ACM instruments was used in this case. Removal of the DC trend from the raw noise data was the first step in the noise analysis when needed. To accomplish this, a least square fitting method was used. Finally, the noise resistance,  $R_n$ , was then calculated as the ratio of the potential noise standard deviation,  $\sigma_v$ , over the current noise standard deviation,  $\sigma_i$ , according to Eq. [1].

### 3. RESULTS AND DISCUSSION.

The effect of carboxyethylimidazoline concentration in the polarization curves of X-120 steel in  $H_2S$ -containing 3 % NaCl solution at 50 °C is shown in Fig.2.

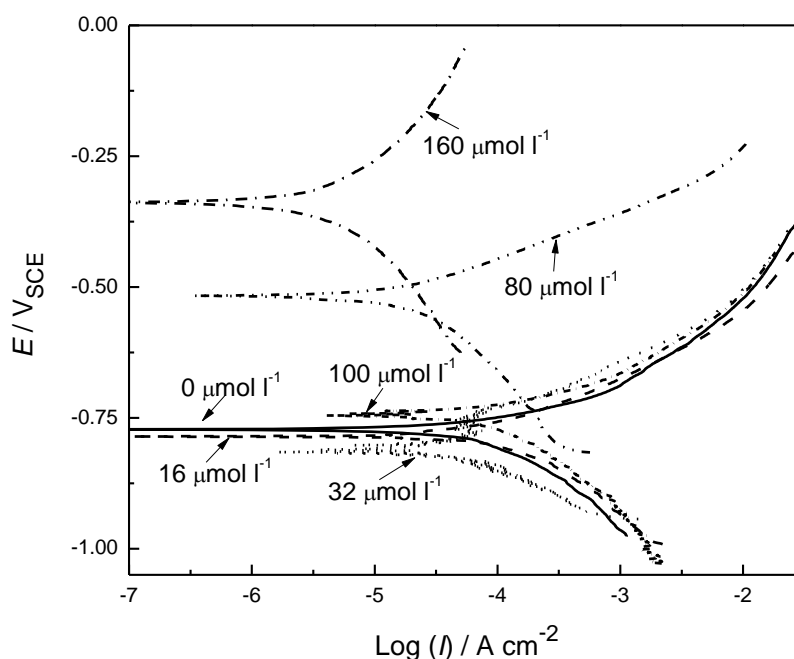


**Figure 2.** Effect of carboxyethylimidazoline concentration in the polarization curves for X-120 steel in  $H_2S$ -containing 3% NaCl solution.

In all cases, the steel shows only an active behavior, anodic dissolution, without evidence of a passive layer. The shape of the curve practically remains the same with the addition of either 16 or 32,

$\mu\text{mol l}^{-1}$  of carboxyethyl-imidazole. The  $E_{\text{corr}}$  value for all the inhibitor concentrations lies between -815 and -755  $\text{mV}_{\text{SCE}}$ , except for 80 and 160  $\mu\text{mol l}^{-1}$  which have  $E_{\text{corr}}$  values of -516 and -340  $\text{mV}_{\text{SCE}}$  respectively. The corrosion current density values,  $I_{\text{corr}}$ , lies between 6 and 200  $\text{nA cm}^{-2}$  respectively. The lowest corrosion rate and noblest  $E_{\text{corr}}$  values are obtained with 160  $\mu\text{mol l}^{-1}$  of carboxyethylimidazole, although a significant reduction in the corrosion rate is reached with the addition of 80  $\mu\text{mol l}^{-1}$  of carboxyethylimidazole, obtaining an  $I_{\text{corr}}$  value of 40  $\text{nA cm}^{-2}$ . Table 2 summarizes the electrochemical values obtained from polarization curves. Table 2 and Fig. 3 show that the lowest corrosion rate is obtained by adding 160  $\mu\text{mol l}^{-1}$  of carboxyethylimidazole. Lower or higher inhibitor concentrations reduces the inhibitor efficiency.

**Table 2.** Electrochemical parameters obtained from polarization curves in the  $\text{H}_2\text{S}$ -containing 3% NaCl solution

Inhibitor concentration ( $\mu\text{mol l}^{-1}$ )	$E_{\text{corr}}$ / $\text{mV}_{\text{SCE}}$	$I_{\text{corr}}$ $\text{nA cm}^{-2}$	$\eta$ / %
0	-774	200	—
16	-785	90	55
32	-814	80	60
80	-516	40	80
160	-340	6	97
332	-743	150	25

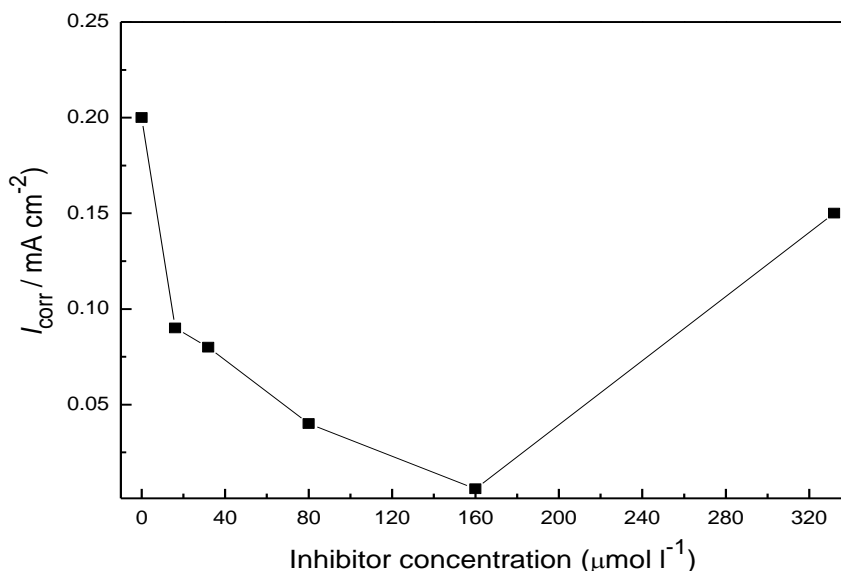


**Figure 3.** Effect of carboxyethylimidazole concentration in the  $I_{\text{corr}}$  value for X-120 steel in  $\text{H}_2\text{S}$ -containing 3% NaCl solution.

The change in the  $R_p$  values with time for X-120 steel in the  $H_2S$ -containing 3% NaCl solution as a function of carboxyethylimidazoline concentration is shown on Fig. 4. It can be seen that the highest  $R_p$  value and thus the lowest  $I_{corr}$  value, is obtained with  $160 \mu\text{mol l}^{-1}$  of carboxyethylimidazoline, remaining more or less constant as time elapses. On the other hand, the lowest  $R_p$  is obtained for the blank, uninhibited solution.

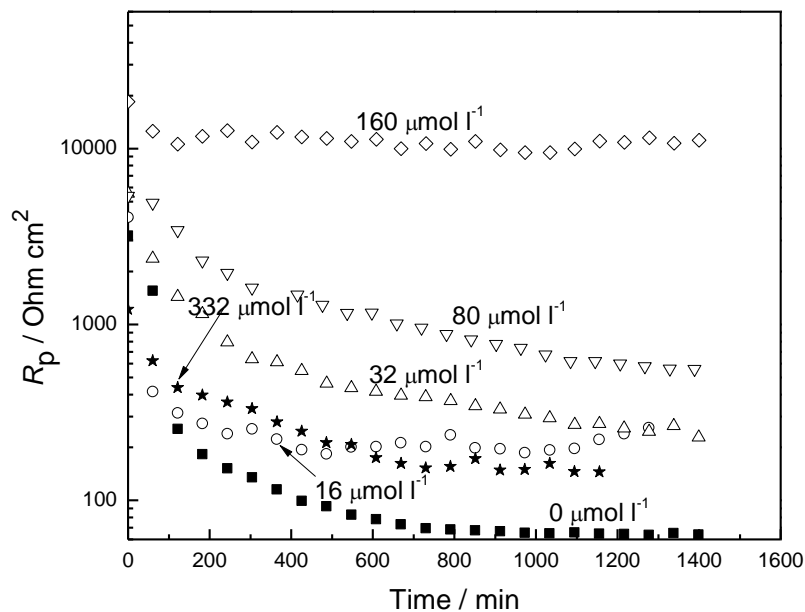


**Figure 4.** Effect of carboxyethylimidazoline concentration on the change in the  $R_p$  value with time for X-120 steel in  $H_2S$ -containing 3% NaCl solution.

All the  $R_p$  values decrease with time, except that for  $160 \mu\text{mol l}^{-1}$  of carboxyethylimidazoline. In solutions containing  $H_2S$ , the corrosion process of iron and carbon steel is generally accompanied by the formation of an iron sulfide film [19, 20]. The fact that  $R_p$  decreases with time, suggests the non-protective nature of the corrosion products film. This film is a non-adherent layer which can be easily removed from the steel surface and can not passivate the steel surface under the environmental conditions used here. The protectiveness of the inhibitor film depends, among other factors, upon the adherence and stability of the inhibitor on this iron sulfide film. Generally speaking, it has been accepted that organic inhibitors form a protective layer on the surface of the metal. However, the decrease in the  $R_p$  value shows that this film inhibitor is unstable and detached from the metal surface, except for  $160 \mu\text{mol l}^{-1}$  carboxyethylimidazoline, where the film formed by inhibitor is more stable.

Nyquist data for the X-120 steel in the uninhibited  $H_2S$ -containing 3 % NaCl solution is shown in Fig. 5. The impedance spectra show one capacitive like, depressed semicircle at high frequency values, and a second semicircle at intermediate and lower frequency values. The high frequency semicircle is related to the double electrochemical layer, whereas the second, lower frequencies semicircle represents the sulfide iron film. In such a process, the high frequency semicircle diameter, which is the charge transfer resistance,  $R_{ct}$ , is equivalent to the linear polarization resistance value,  $R_p$ .

The semicircle diameter increases during the first hours but after this time it decreases in the same way as  $R_p$  did in Fig. 4. The fact that the semicircle diameter increases first and after a while it decreases suggests the non-protective nature of the corrosion products film. However, after a few hours, the semicircle diameter decrease as time elapses, indicating an increase in the corrosion rate.

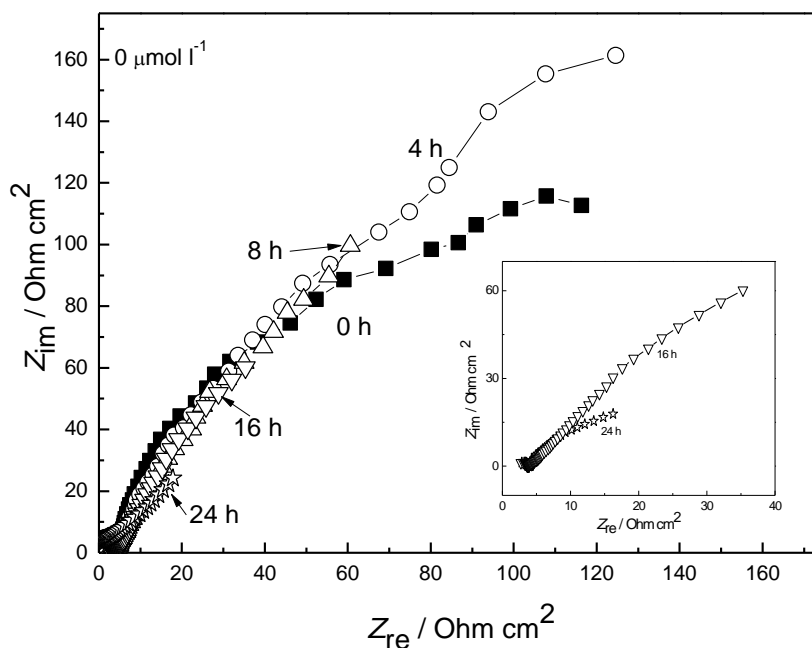


**Figure 5.** Nyquist diagram for X-120 steel in uninhibited  $H_2S$ -containing 3% NaCl solution.

In  $H_2S$ -containing solutions, the corrosion process of iron and steel is generally accompanied by the formation of an iron sulfide film [3-5, 21-22]. Thus, the increase in impedance is due to the growth of this iron sulfide film. The decrease in the semicircle diameter, and thus the impedance, indicates that film growth continues until a critical thickness, after which the film cracks and is detached from the metal surface. This is in agreement with the results reported by Vedage et al. [22] for 4130 steel in  $H_2S$  solution at 95 °C, finding that the corrosion process for short times is film diffusion limited, whereas for longer times a steady state was reached at which the film growth was balanced by its dissolution into the aqueous phase, leading to a limited film thickness. Wuang et al. [23], working with carbon steel in  $H_2S$  solution at 25 °C reports at an early stage one large semicircle with its impedance increasing with time. At a later stage, the precipitation of sulfide film revealed the presence of a second capacitive semicircle at lower frequency values. In a similar way, Arzola et al [24], working with X-70 pipeline steel in a  $H_2S$ -containing 3 wt. % NaCl solution at 25 °C, reports that the Nyquist diagrams shows the presence of one loop at high frequencies and an uncompleted loop at lower frequencies. However, when used the 3% NaCl solution under dynamic conditions, using 1000 rpm in a rotating disc electrode, only one capacitive-like semicircle is found, similar to the one found in this work. Under static conditions, the increase in the semicircle diameter value with time during the first hours has been reported [24] to be due to the growth of an iron sulfide film, whereas the decrease in the semicircle diameter was related to the dissolution of this film.



The effect of carboxyethylimidazoline concentration in the Nyquist diagrams X-120 steel is shown in Fig. 6.

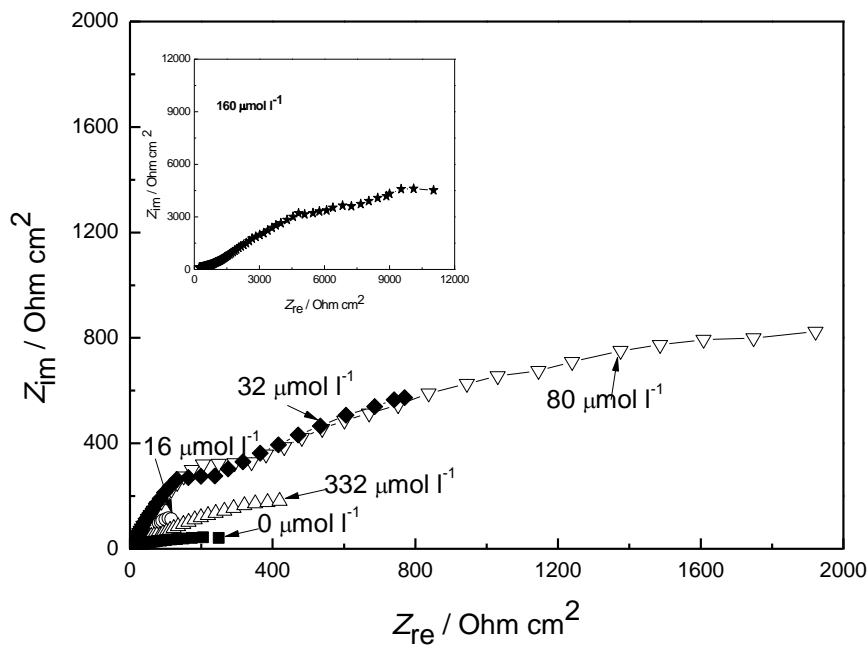


**Figure 6.** Effect of carboxyethylimidazoline concentration in the Nyquist diagrams for X-120 steel immersed in H<sub>2</sub>S-containing 3% NaCl solution.

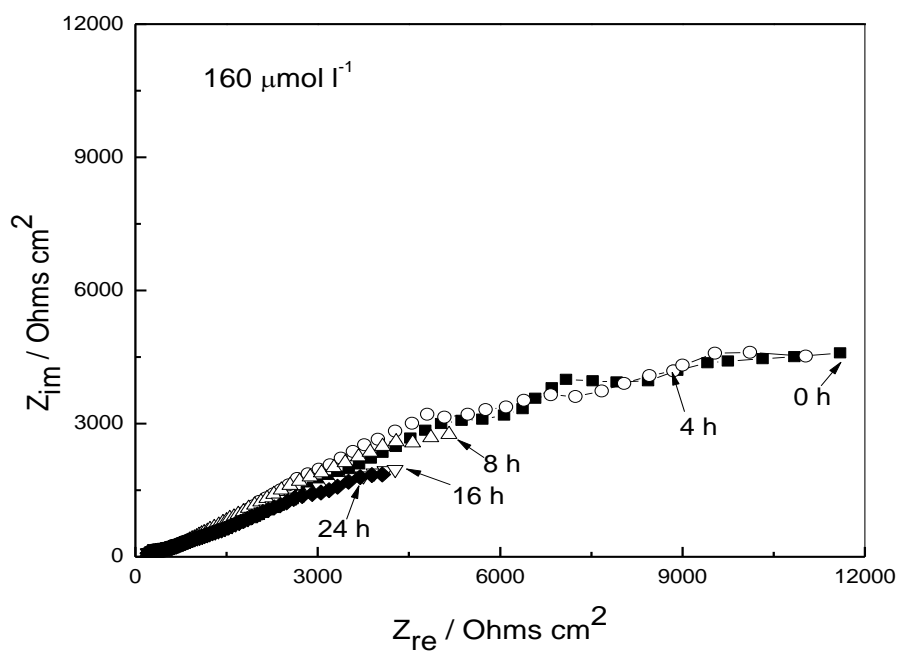


**Figure 7.** Nyquist diagram for X-120 steel in H<sub>2</sub>S-containing 3% NaCl solution with 160 μmol/l of carboxyethylimidazoline.

It can be seen that, in all cases, except for the addition of 160  $\mu\text{mol/l}$  of carboxyethylimidazoline, the data describes a depressed, capacitive-like, semicircle at high frequency values and second semicircle at intermediate frequencies, similar to that shown by uninhibited solution in Fig. 5. When 160  $\mu\text{mol l}^{-1}$  of carboxyethylimidazoline are added, a third semicircle emerges at lower frequencies, Fig. 7, which is attributed to an inhibitor-formed film. In this case, the semicircle diameter remains more or less constant during the first hours, but after this time, the semicircle diameter decreases with time, indicating an increase in the corrosion rate. According to Ramachandran et al. [14] the film formed by the presence of long hydrocarbon chains in the structure of the imidazoline acts as a protective barrier against aggressive ions from the bulk solution. The change in the impedance modulus with time for the different inhibitor concentrations,  $[Z]$ , is shown in Fig. 8. It can be seen that the highest  $[Z]$  value is for an inhibitor concentration of 160  $\mu\text{mol/l}$ , whereas the lowest value is for the uninhibited solution. Regardless of the inhibitor concentration, the  $[Z]$  value decreases with time. This behavior is similar to that shown by  $R_p$ , Fig. 4, where the highest inhibitor efficiency was obtained by adding 160  $\mu\text{mol/l}$  of carboxyethylimidazoline.

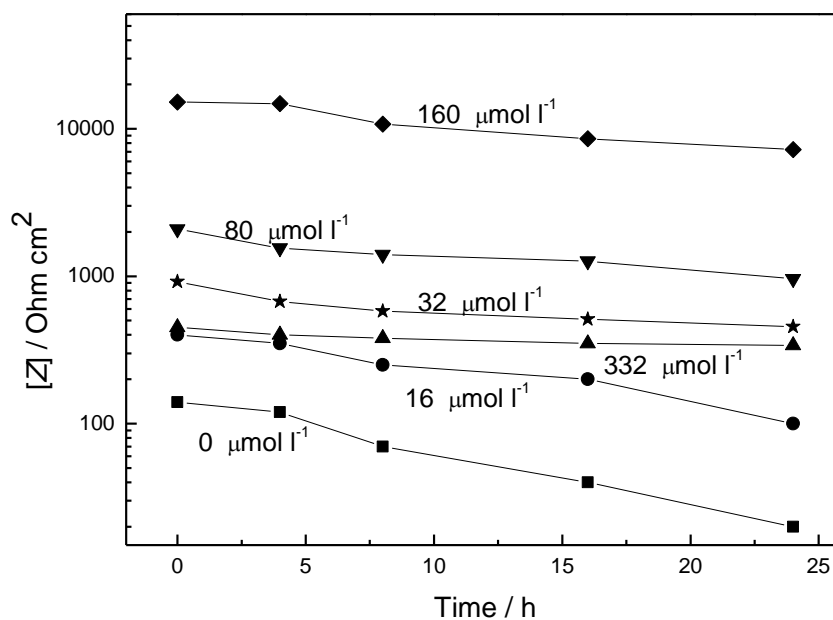


**Figure 8.** Effect of carboxyethylimidazoline concentration on the change in the impedance modulus values with time,  $[Z]$ , for X-120 steel in  $\text{H}_2\text{S}$ -containing 3% NaCl solution.

The use of electrochemical noise can give information about the type of corrosion, either localized or uniform, that an alloy can be susceptible to. The noise in current for X-120 steel in the uninhibited  $\text{H}_2\text{S}$ -containing 3% NaCl solution after different exposure times is shown in Fig. 9. At the beginning of the experiment, the time series describes transients of high intensity and high frequency, typical of a material undergoing uniform corrosion. After 4 hours of exposure, both the intensity and frequency of the transients decrease dramatically; these transients are due to the breakdown of any film

formed on the steel surface, leaving it unprotected in some places, indicating that the material is now susceptible to a localized type of corrosion such as pitting.

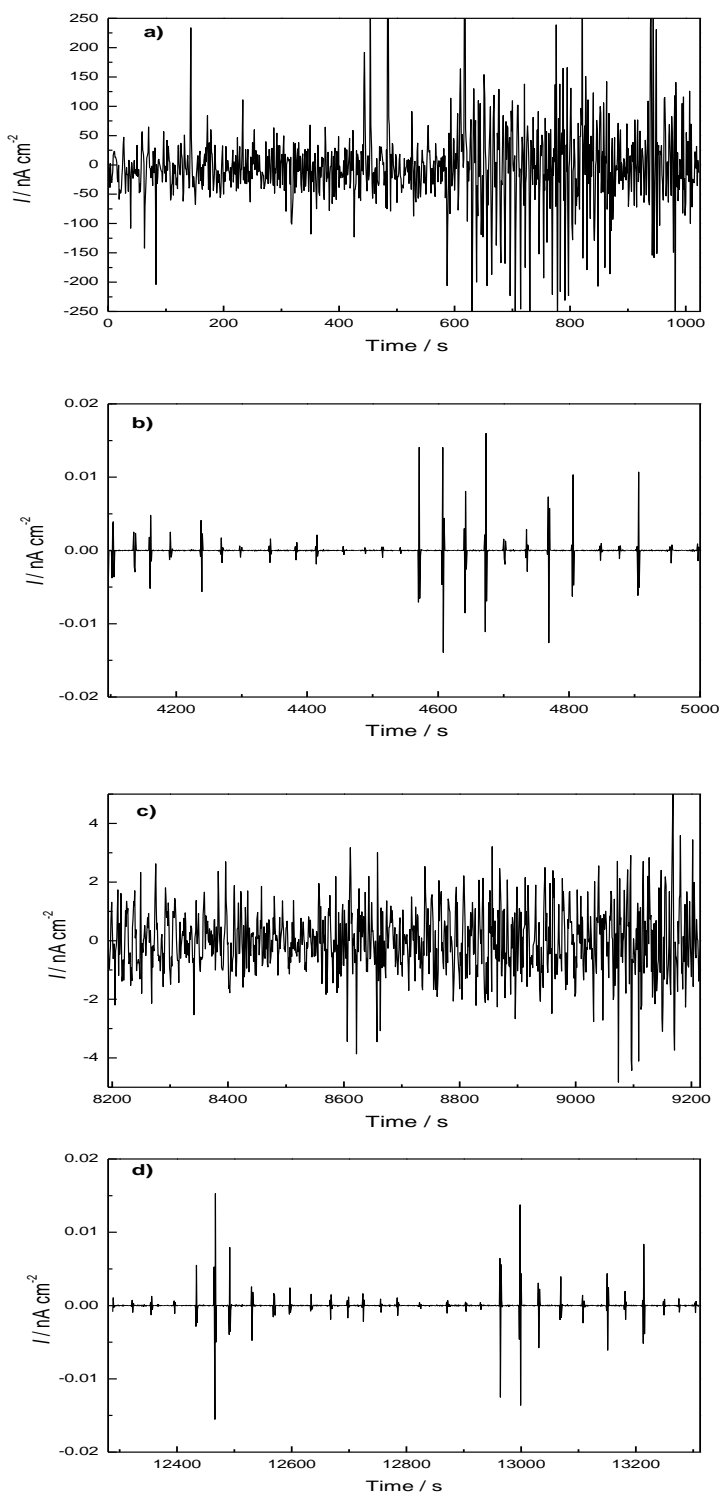


**Figure 9.** Noise in current for X-120 steel in uninhibited H<sub>2</sub>S-containing 3% NaCl solution after a) 0, b) 4 , c) 8 and d) 12 hours of exposure.

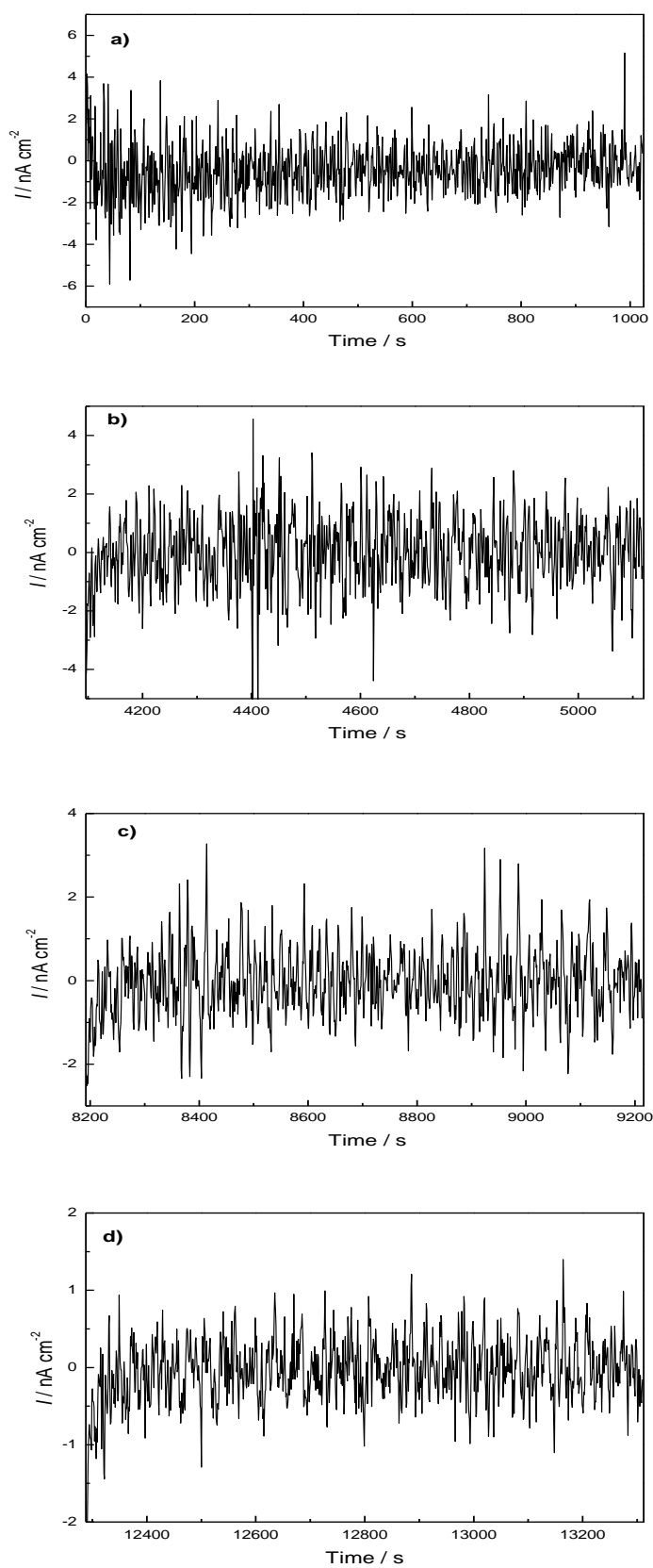


**Figure 10.** Noise in current for X-120 steel in H<sub>2</sub>S-containing 3% NaCl solution containing 160 μmol l<sup>-1</sup> of carboxyethylimidazoline after a) 0, b) 4, c) 8 and d) 12 hours of exposure

Thus, Fig. 9 shows that the iron sulfide is formed, but after some time it cracks and is detached from the steel surface. Unlike this, time series for X-120 steel exposed to the inhibited  $\text{H}_2\text{S}$ -containing solution with  $160 \mu\text{mol l}^{-1}$  of carboxyethylimidazoline, Fig. 10, shows transients of high frequency and low intensity, indicating that during all the testing times the steel is susceptible only to a uniform type of corrosion, and thus, that any film formed by the inhibitor is very stable with time and protects the steel against corrosion.

There is a factor called ‘‘Localization Index,  $LI$ ’’ defined as:

$$LI = \frac{\sigma_i}{i_{rms}} \quad [4]$$

where  $\sigma_i$  is the current noise standard deviation and  $i_{rms}$  the current root mean square value [25] which establishes that for  $LI$  values between 1 and 0.1, the type of corrosion that the material suffers is localized, when the  $LI$  value lies between 0.1 and 0.01, there is a mixture of both uniform and localized types of corrosion; finally, for  $LI$  values between 0.01 and 0.001, there is a tendency towards a uniform type of corrosion.

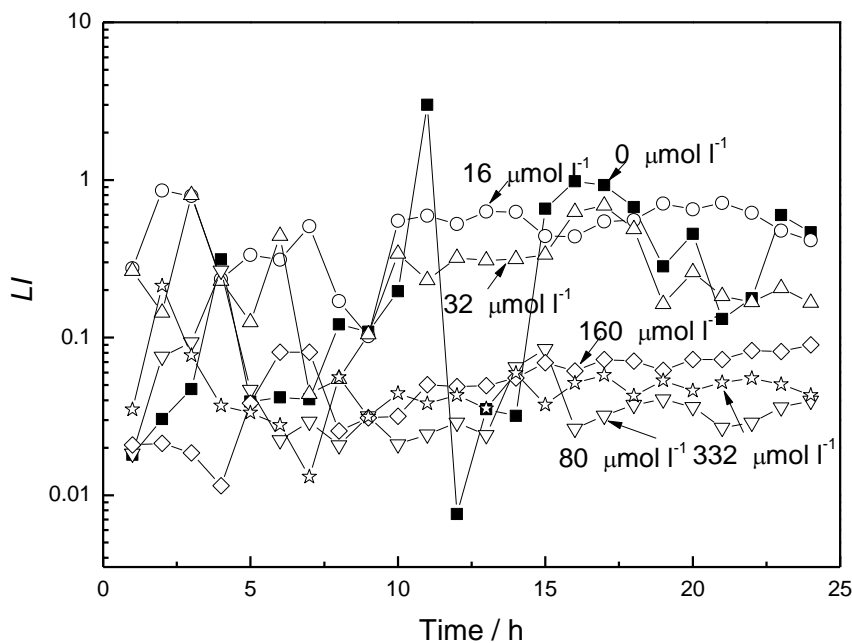


**Figure 11.** Change in the localization index factor with time,  $LI$ , for the different carboxyethylimidazoline concentrations

Fig. 11 shows the effect of carboxyethylimidazoline concentration in the  $LI$  values for X-120 steel as a function of time. Fig. 11 shows that for inhibitor concentrations lower than  $32 \mu\text{mol l}^{-1}$  the steel is very susceptible to a localized type of corrosion, whereas for inhibitor concentrations equal or higher than  $80 \mu\text{mol l}^{-1}$ , the steel is more susceptible to uniform type corrosion. For uninhibited

solution, it can be seen that for times lower than 15 hours, the  $LI$  value fluctuates drastically with time, indicating that sometimes the steel is very susceptible to a localised type of corrosion but some other times it is susceptible to a uniform type of corrosion. As it was indicated above, this is due to the fact that the iron sulfide film cracks and is detached from the steel surface, leaving unprotected some parts of the steel from the aggressive environment. For inhibitor concentrations equal to  $80 \mu\text{mol l}^{-1}$ , the inhibitor must form a protective, stable film, decreasing the susceptibility towards both localized and uniform corrosion. Once the inhibitor concentration reaches a value of  $160 \mu\text{mol l}^{-1}$ , the highest inhibitor efficiency is reached as shown by the LPR measurements, Fig.4.

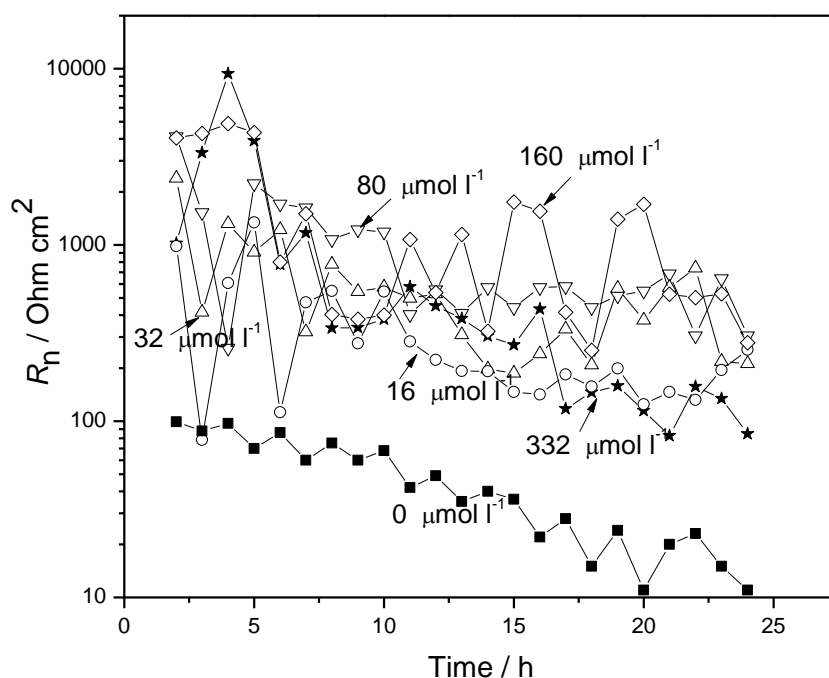


**Figure 12.** Effect of carboxyethylimidazoline concentration on the change in the  $R_n$  values with time for X-120 pipeline steel in the  $\text{H}_2\text{S}$ -containing 3% NaCl solution.

The combined effect of potential standard deviation,  $\sigma_v$ , and current standard deviation,  $\sigma_i$ , results in the noise resistance value,  $R_n$ , (eq. [1]) which is inversely proportional to the corrosion rate,  $I_{corr}$ , as previously done with  $R_p$ , Fig. 4. An estimation of the corrosion rate can be completed through the variation of  $R_n$  with time for the different inhibitor concentrations, as can be seen in Fig. 12. This behavior is very similar to that observed in Fig. 4 by  $R_p$  and  $[Z]$  in Fig. 8: high values at the beginning of the test and then a decrease in the value towards the end of the test. As can be seen, initially  $R_n$  was high and corresponds to a low corrosion rate. Likewise, low  $R_n$  observed towards the end of testing corresponds to an increase in the corrosion rate. This shows that the film formed by the inhibitor remains on the metal surface during a short period of time, i.e. it has a short time of residence. As it can be seen, the highest  $R_n$  value is obtained with the addition of  $160 \mu\text{mol l}^{-1}$  of carboxyethylimidazoline, whereas the lowest  $R_n$  value was obtained for the blank solution. Thus,

corrosion rates estimated by polarization curves, LPR and EIS measurements were very similar to those obtained by EN measurements, which establishes that the optimum carboxyethylimidazoline concentration in the H<sub>2</sub>S-containing 3% NaCl solution at 50 °C is 160 μmol l<sup>-1</sup>.

#### 4.CONCLUSIONS

The effect of carboxyethylimidazoline concentration on the H<sub>2</sub>S corrosion inhibition of API X-120 steel in 3% NaCl solution at 50 °C has been studied using different electrochemical techniques. Different techniques showed that the best corrosion inhibition was obtained by adding 160 μmol/l of carboxyethylimidazoline reaching an efficiency value of 97%. For all the inhibitor concentrations this efficiency decreased as time elapsed indicating a short time of residence of the film formed inhibitor except for 160 μmol l<sup>-1</sup>, where the film formed was more stable. The steel was very susceptible towards a localized type of corrosion for inhibitor concentrations lower than 80 μmol l<sup>-1</sup>, but above this inhibitor concentration, the steel was more susceptible towards a uniform type of corrosion.

#### References

1. L. Quej-Aké, R. Cabrera-Sierra, E. Arce-Estrada, J. Marin-Cruz, *Int. J. Electrochem. Sci.* 3 (2008) 56.
2. S.D. Kapusta, B.F.M. Pots, "The Materials and Corrosion View of Wet Gas Transportation", in: *Advances in Corrosion Control and Materials in Oil and Gas Production Edited by P. S. Jackman and L. M. Smith* European Federation of Corrosion Publications 26 (1998) 5.
3. M.B. Kermani, A. Morshed, *Corrosion* 59(2003) 659.
4. H.Y. Ma, X.L. Cheng, G.Q. Li, S.H. Chen, Z.L. Quan, S.Y. Zhao, L. Niu, *Corros. Sci.* 42 (2010)1669.
5. E Abelev, J. Sellberg, T.A. Ramanarayanan, S.L. Bernasek, *J. Mat. Sci.* 44 (2009) 6167.
6. S.A.Abd El-Maksoud, *Int. J. Electrochem. Sci.*, 3 (2008) 528.
7. J.W. Tang, Y.W. Sha, J.B. Guo, T. Zhang, G.Z. Meng, F.H. Wang, *Corros. Sci.* 52 (2010) 2050.
8. S.N. Smith "A Proposed Mechanism for Corrosion in Slightly Sour Oil and Gas Production". *Poc. 12<sup>th</sup> Int. Corrosion Congress held in September 19-23 Houston, TX, (1993) NACE International.*
9. F. Farelas, A. Ramirez, *Int. J. Electrochem. Sci.* 5 (2010) 797.
10. J. G. Gonzalez-Rodriguez, T. Zeferino-Rodriguez D.M. Ortega, S.A. Serna, B. Campillo, E. Valenzuela, J. A. Juárez-Islas, *Int. J. Electrochem. Sci.* 2 (10) (2007) 883.
11. S. Ramachandran, V. Jovancevic, *Corrosion* 55 (1999) 259.
12. Z. Xueyuan, *Corros. Sci.* 43 (2001) 1417.
13. F. Bentiss, M. Lagrenee, M. Traisnel, J.C. Hornez, *Corros. Sci.* 41 (1999) 789.
14. S. Ramachandran, M. Tsai, M. Blanco, H. Chen, W.A. Tang, *Langmuir* 12 (1996) 6419.
15. D. Wang, S. Li, M. Ying, M. Wang, Z. Xiao, Z. Chen, *Corros. Sci.* 41 (1999) 1911.
16. A.Popova, S. Raicheva, E. Sokolova, M. Christov, *Langmuir* 12 (1996) 2083.
17. L. Nykos, T. Pajlossy, *Electrochim. Acta* 30 (1985)1533.
18. E. Garcia-Ochoa, J. Genesca *J. Surf. and Coat. Technol.* 184 (2004) 322.
19. E. Sarmiento-Bustos, J.G. González Rodriguez, J. Uruchurtu, G. Dominguez-Patiño, V.M. Salinas-Bravo, *Corros. Sci.* 50 (2008) 2296.
20. P.H. Tewart, A.B. Campbell, *Can. J. Chem.* 57 (1979)188.
21. F.H.Meyer, O.L. Riggs, R.L. McGlasson, J.D.Sudbury, *Corrosion* 14 (1958) 69.

22. H. Vedage, T.A. Ramanarayanan, J.D. Mumford, S.N. Smith, *Corrosion* 49 (1993)114.
23. H.H. Wang, W.T. Tsay, J.T. Lee, *Electrochim Acta* 41 (1996)1191.
24. S. Arzola, J. Mendoza-Florez, R. Duran-Romero, J.Genesca, *Corrosion* 62 (2006) 433.
25. D. Eden, "Electrochemical Noise-The First Two Octaves-Part I", *Corrosion'1988*, National Association of Corrosion Engineers, Houston, TX, (1998) Paper No. 386.